

See discussions, stats, and author profiles for this publication at: <https://www.researchgate.net/publication/275525661>

# One-Pot Synthesis of Brightly Fluorescent Mes 2 B-Functionalized Indolizine Derivatives via Cycloaddition Reactions

ARTICLE in ORGANIC LETTERS · APRIL 2015

Impact Factor: 6.36 · DOI: 10.1021/acs.orglett.5b00994 · Source: PubMed

CITATION

1

READS

38

7 AUTHORS, INCLUDING:



Dengtao Yang

Queen's University

11 PUBLICATIONS 56 CITATIONS

SEE PROFILE



Soren K. Mellerup

Queen's University

8 PUBLICATIONS 6 CITATIONS

SEE PROFILE



Xiang Wang

Queen's University

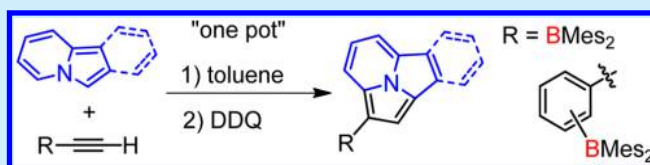
10 PUBLICATIONS 25 CITATIONS

SEE PROFILE

One-Pot Synthesis of Brightly Fluorescent Mes<sub>2</sub>B-Functionalized Indolizine Derivatives via Cycloaddition ReactionsDeng-Tao Yang,<sup>†</sup> Julian Radtke,<sup>‡</sup> Soren K. Møllerup,<sup>†</sup> Kang Yuan,<sup>†</sup> Xiang Wang,<sup>†</sup> Matthias Wagner,<sup>\*,‡</sup> and Suning Wang<sup>\*,†</sup><sup>†</sup>Department of Chemistry, Queen's University, Kingston, Ontario K7L 3N6, Canada<sup>‡</sup>Institut für Anorganische und Analytische Chemie, Goethe-Universität Frankfurt, Max-von-Laue-Strasse 7, D-60438 Frankfurt am Main, Germany

## S Supporting Information

**ABSTRACT:** Four new BMes<sub>2</sub>-functionalized indolizine derivatives (Mes = mesityl) have been prepared via the cycloaddition reaction between pyrido[2,1-*a*]isoindole (A) or pyrrolo[1,2-*a*]pyridine (B) and BMes<sub>2</sub>-containing alkynes. All four compounds are brightly blue or blue-green fluorescent with  $\lambda_{\text{em}} = 428\text{--}495\text{ nm}$  and  $\Phi = 0.27\text{--}0.68$ , depending on the substitution position of the BMes<sub>2</sub> group. Experimental and TD-DFT computational data indicated that the primary electronic transitions responsible for the fluorescence of 1–4 are from HOMO to LUMO ( $\pi \rightarrow \pi^*$ ) rather than charge transfer from N  $\rightarrow$  B, which is in agreement with previous findings suggesting that the lone-pair on N is delocalized throughout the N-heterocycles.



Luminescent materials based on  $\pi$ -conjugated aromatic systems have long been studied for many different applications such as organic light emitting diodes (OLEDs),<sup>1</sup> organic field effect transistors (OFETs),<sup>2</sup> and fluorescent probes/sensors.<sup>3</sup> Within this vast family of organic compounds, two N-heterocycles, namely pyrido[2,1-*a*]isoindole (A) and pyrrolo[1,2-*a*]pyridine (B), have started to attract some attention over the past decade due to their interesting electronic structure which allows them to undergo 1,3-dipolar cycloadditions with alkynes and ultimately expand their  $\pi$ -system through subsequent dehydrogenation yielding indolizino[3,4-*ab*]isoindole and pyrrolo[2,1,5-*cd*]indolizine derivatives, respectively.<sup>4</sup> This strategy has been employed to great effect with respect to purely organic fluorophores, where certain cycloaddition products obtained using electron poor alkynyl-dipolarophiles possessed good fluorescent quantum efficiencies and blue light emission.<sup>4a</sup> Aside from extending aromatic  $\pi$ -networks, incorporating three-coordinated organoboron moieties into such molecules can also have a dramatic effect on their electronic structure and photophysical properties<sup>5</sup> due to boron's empty  $p_z$  orbital that becomes part of the  $\pi$ -system. Previously, it has been shown that triarylboron containing donor–acceptor systems tend to possess large electronic dipoles, which often results in enhanced donor–acceptor charge transfer (CT) upon photoexcitation and has shown significant promise as selective sensors for anions such as fluoride or cyanide.<sup>6</sup> Our interest in A arose as part of our recent work with B,N-heterocycles, where A was found to be a product of their retro-1,1-hydroboration.<sup>7</sup> Given the potential of electron-rich A/B to act as suitable donors, we set out to create new boron-appended fluorophores through the cycloaddition of A/B with dimesitylboron functionalized alkynes with the aim of generating new CT fluorescent molecules (1–4, Scheme 1). Much to our surprise, these new species do not

Scheme 1. Synthetic Procedures of Mes<sub>2</sub>B-Functionalized Indolizine Derivatives 1–4

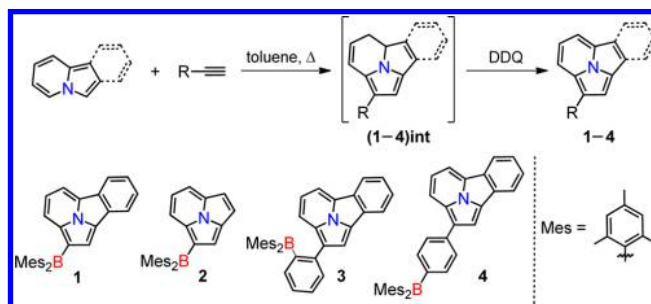


exhibit CT emission but rather intense  $\pi \rightarrow \pi^*$  transitions, which emit either blue or blue-green light as discussed in further detail below.

Compound A<sup>8a</sup> and the alkyne starting materials BMes<sub>2</sub>-acetylene,<sup>8b</sup> *o*-BMes<sub>2</sub>-C<sub>6</sub>H<sub>4</sub>-acetylene,<sup>8c</sup> and *p*-BMes<sub>2</sub>-C<sub>6</sub>H<sub>4</sub>-acetylene<sup>8d</sup> were prepared according to literature methods. The cycloaddition reaction of the alkyne compounds with compounds A or B was carried out in toluene under nitrogen according to the procedure shown in Scheme 1. The cycloaddition between A and BMes<sub>2</sub>-acetylene proceeded rapidly, yielding 1-int quantitatively after 1 h at room temperature. Although 1-int can be isolated and purified prior to dehydrogenation,<sup>9</sup> the subsequent addition of 2,3-dichloro-5,6-dicyano-1,4-benzoquinone (DDQ, 1.2 equiv), a well-known reagent for oxidative dehydrogenation,<sup>10</sup> to the reaction mixture was found to be the most efficient method of generating compound 1 in

Received: April 6, 2015

excellent yield (i.e., a one-pot synthesis). With respect to the synthesis of **2–4**, their initial cycloaddition reactions required refluxing the N-heterocycles and the corresponding alkyne starting material in toluene for several days due to the relatively low reactivity of **B** and  $\text{BMes}_2\text{-C}_6\text{H}_4$ -alkynes. Under these harsher reaction conditions, both the intermediates (**int**) and the fully dehydrogenated products **2–4** were observed. Therefore, no attempts to isolate the intermediates were performed as it would have resulted in a loss of potential yield. Once again, addition of DDQ to each reaction mixture resulted in quantitative conversion to the desired products **2–4** in decent to good yield. In the previously reported cycloaddition reactions of **A** with alkynes, the most commonly used dehydrogenation reagent is sulfur,<sup>4a</sup> which requires the isolation of the intermediate first. Our attempts employing sulfur powder as the oxidant for converting the intermediate **1-int** to **1** required much longer reaction times and elevated temperatures compared to DDQ. Furthermore, we were unable to fully remove the excess sulfur from the final products via recrystallization or column/thin-layer chromatography. The one-pot procedure employing DDQ as the oxidant not only greatly simplifies the reaction but also allows us to isolate the fully conjugated products in high purity and good yield. Compounds **1–4** and **1-int** were fully characterized by  $^1\text{H}$  and  $^{13}\text{C}$  NMR as well as HRMS.<sup>9</sup> Attempts to record the  $^{11}\text{B}$  NMR spectra for these compounds at various temperatures have not been successful.

$^1\text{H}$  NMR data reveals that only one regioisomer is formed for **1–4**, in which the carbon atom of the alkyne that is attached to the boron unit forms a bond with a pyridyl carbon atom. The regioselectivity of the cycloaddition reaction is further supported by the single-crystal X-ray diffraction data of compounds **1**, **1-int**, and **3**. The crystal structures of **1** and **3** are shown in Figure 1, and

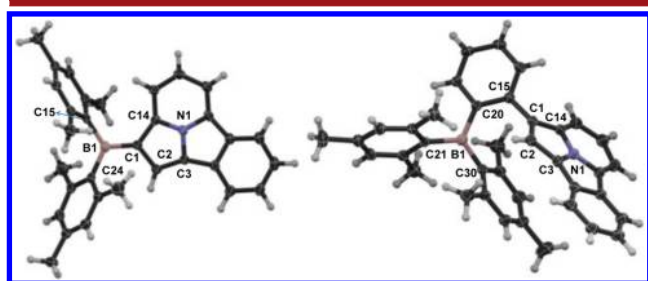


**Figure 1.** Crystal structure of **1** (left) and **3** (right). Important bond lengths (Å) for **1**: B(1)–C(1) 1.520(3), B(1)–C(15) 1.596(3), B(1)–C(24) 1.588(4), C(1)–C(2) 1.441(3), C(1)–C(14) 1.440(3), C(2)–C(3) 1.379(3), N(1)–C(3) 1.379(3), N(1)–C(14) 1.366(3); for **2**: B(1)–C(20) 1.572(3), B(1)–C(21) 1.576(3), B(1)–C(30) 1.580(3), C(1)–C(2) 1.403(3), C(1)–C(14) 1.421(3), C(2)–C(3) 1.406(3), N(1)–C(3) 1.357(2), N(1)–C(14) 1.373(2).

that of **1-int** is provided in the Supporting Information. The observed regioselectivity of the 1,3-dipolar cycloaddition is in agreement with the frontier molecular orbital theory,<sup>11</sup> which rationalizes that the dominant electronic interaction is the combination of the largest HOMO and LUMO orbital contributions from the 1,3-dipole and dipolarophiles, respectively. From our computational analysis,<sup>9</sup> the C(6) position of **A** (labeled as C(3) in the crystal structure) and C(3) position of **B** were found to possess the largest HOMO contribution, while the terminal alkyne carbon of all three dipolarophiles were found to possess the largest LUMO contribution which ultimately leads to the formation of only one regioisomer.

Although molecules of **1** form discrete  $\pi$ -stacked dimers between each indolizino[3,4,5-*ab*]isoindole ring in the crystal lattice (Figure 2), no extended  $\pi$ -stacking interactions were

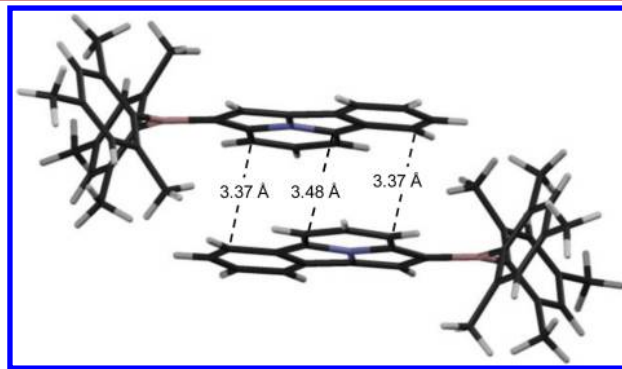


**Figure 2.**  $\pi$ -Stacked dimer of **1**.

observed. This is in sharp contrast to previously reported indolizino[3,4,5-*ab*]isoindole derivatives, which display strong and extended  $\pi$ -stacking interactions in the solid state.<sup>4a</sup> The bulky  $\text{BMes}_2$  group is clearly responsible for the significant reduction in intermolecular  $\pi$ -stacking interactions of molecule **1**. It is conceivable that similar  $\pi$ -stacking interactions are also possible for molecules **2** and **4** due to their structural similarity to **1**. Molecules of **3** display intramolecular  $\pi$ -stacking interactions between the five-membered ring containing the C(1), C(2), C(3), and C(14) atoms and the benzene ring of a mesityl with atomic separation distances of 3.10 (C(1)⋯C(30)) to 3.90 Å (Figure 1), which is attributed to steric congestion. Intermolecular  $\pi$ -stacking interactions similar to that of **1** were not observed for **3**.

The attachment of the  $\text{BMes}_2$  group to indolizino[3,4,5-*ab*]isoindole has a distinct impact on the electronic and photophysical properties of the molecule. Molecules **1–4** display pseudo-reversible reduction peaks between  $-2.34$  V (**2**) and  $-2.55$  V (**3**) (vs.  $\text{Cp}_2\text{Fe}/\text{Cp}_2\text{Fe}^+$ ), which are characteristic of the boron unit but somewhat more negative than those of  $\text{BMes}_2\text{Ar}$  (Ar = phenyl or substituted phenyl)<sup>12</sup> due to the electron-rich nature of the indolizino[3,4,5-*ab*]isoindole or pyrrolo[2,1,5-*cd*]indolizine N-heterocycle. An irreversible oxidation peak is also observed for all four compounds between 0.53 (**3**) and 1.00 (**2**) V, which is characteristic of the N-heterocyclic unit.<sup>4a</sup>

Much like the nonboron-containing parent molecules, **1–4** all possess strong absorption bands between 400 and 500 nm as shown in Figure 3 and Table 1. As one might expect, the absorption bands of **1** and **2** are hypsochromically shifted by  $\sim 40$  nm compared to **3** and **4**, which is most likely due to the

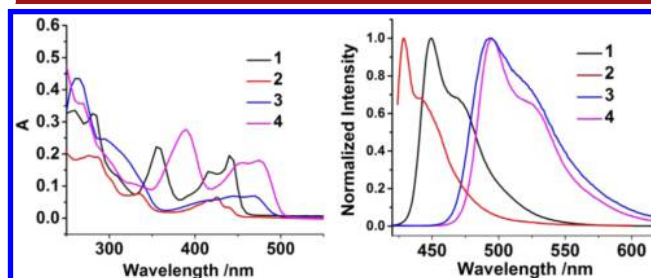


**Figure 3.** UV-vis (left) and emission (right) spectra of compounds **1–4** in  $\text{CH}_2\text{Cl}_2$  ( $1.0 \times 10^{-5}$  M).

Table 1. Absorption and Fluorescence Data

| compd | $\lambda_{\text{abs}}$ (nm) ( $\epsilon$ , M <sup>-1</sup> cm <sup>-1</sup> ) <sup>a</sup> | $\lambda_{\text{em}}$ <sup>b</sup> (nm) | $\Phi$ <sup>c</sup> |
|-------|--|---|---------------------|
| 1     | 355, 415, 440 ( $1.95 \times 10^4$ )   | 448/468                                 | 0.64/0.51           |
| 2     | 335, 415, 425 ( $1.80 \times 10^4$ )   | 428/440, 505                            | 0.27/0.31           |
| 3     | 445, 468 ( $0.692 \times 10^4$ )   | 494/494                                 | 0.33/0.97           |
| 4     | 389, 455, 475 ( $0.656 \times 10^4$ )  | 495/505                                 | 0.68/0.60           |

<sup>a</sup> $10^{-5}$  M in CH<sub>2</sub>Cl<sub>2</sub> at 298 K. <sup>b</sup>CH<sub>2</sub>Cl<sub>2</sub>/PMMA film (10 wt %). <sup>c</sup>The solution QY was determined in CH<sub>2</sub>Cl<sub>2</sub> using 9,10-diphenylanthracene as the reference under N<sub>2</sub>. The solid-state QY was measured using an integration sphere.

increased  $\pi$ -conjugation in the latter. Compared to **4**, the absorption band of **3** is weaker and at a slightly higher energy, which is likely caused by the steric congestion in **3** that results in poor  $\pi$ -conjugation between the phenyl-BMes<sub>2</sub> and indolizino[3,4,5-*ab*]isindolyl ring.

To investigate the origin of the low energy absorption bands and electronic properties of these new molecules, TD-DFT calculations were performed on the computationally optimized geometries of **1–4** and **1**'s parent molecule (**1-no B**). For **1–4**, the predicted UV-vis spectra were found to be in good agreement with the experiment data.<sup>9</sup> For **1**, **2**, and **4**, the low energy absorption band is likely from the S<sub>0</sub> → S<sub>1</sub> electronic transition, which primarily involves HOMO → LUMO (>90%, large oscillator strengths). As shown in Figure 4, the HOMO is

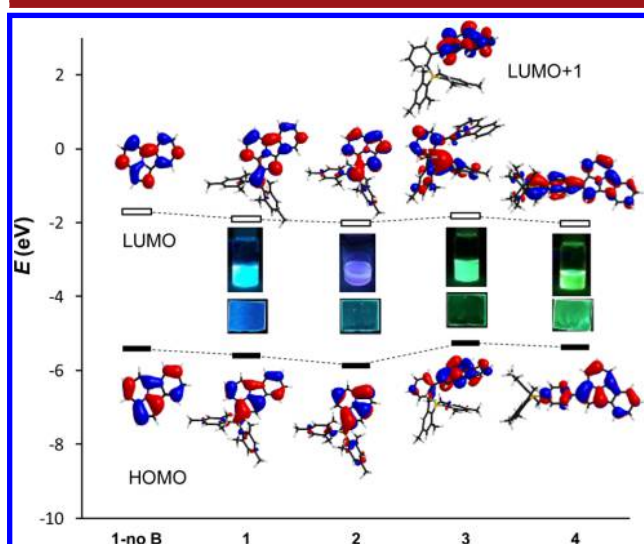


**Figure 4.** Energies and diagrams of HOMO and LUMO (LUMO+1) for the parent molecule (**1-no B**) and **1–4**. Inset: photographs showing the fluorescent colors of **1–4** in CH<sub>2</sub>Cl<sub>2</sub> (top) and PMMA films (10 wt %).

concentrated on the N-heterocyclic ring, while the LUMO is dominated by the empty p<sub>π</sub> orbital of the boron atom and the  $\pi^*$ -orbitals of the N-heterocyclic ring. Therefore, these absorption bands appear to be  $\pi \rightarrow \pi^*$  transitions. With respect to **3**, its low energy absorption band is predicted to be composed of transitions to S<sub>1</sub> and S<sub>2</sub>, which involve HOMO → LUMO and HOMO → LUMO+1, respectively. As with the other three compounds, the HOMO of **3** is comprised of the  $\pi$ -orbitals from the N-heterocyclic ring system. Although the vacant p-orbital on the boron atom also dominates the LUMO of compound **3**, it possesses almost no contribution from the N-heterocyclic ring system. Rather, the remaining contributions to the LUMO of **3** are the  $\pi^*$ -orbitals of both the phenyl linker and mesityls. Therefore, the S<sub>0</sub> → S<sub>1</sub> transition of **3** appears to have CT

character. However, close in energy (5 nm difference) and with a greater oscillator strength is the S<sub>0</sub> → S<sub>2</sub> transition that can be characterized as  $\pi(\text{HOMO}) \rightarrow \pi^*(\text{LUMO}+1)$  localized on the N-heterocycle and likely is the predominant excitation of **3**. The attachment of the BMes<sub>2</sub> unit to the parent molecule (**1-no B**) appears to stabilize both the HOMO and LUMO without significantly changing the HOMO–LUMO gap. The calculated trend of HOMO and LUMO energies agree with our electrochemical data.<sup>9</sup>

All four compounds are brightly fluorescent with the emission energy following the same trend as the absorption spectra (Figure 3). The emission maxima of **1–4** in CH<sub>2</sub>Cl<sub>2</sub> were found to be at 448, 428, 494, and 495 nm, respectively, with **1** and **4** having the most impressive emission quantum efficiencies (0.64 and 0.68, respectively). This indicates that both the N-heterocyclic  $\pi$ -system and appended organoboron moiety play a pivotal role in the electronic structure of these compounds. For **1**, **2**, and **4**, the emission peaks were found to be unaffected by solvents of varying polarity,<sup>9</sup> which is in agreement with the  $\pi \rightarrow \pi^*$  transition localized on the N-heterocycle being the first excited state.<sup>9</sup> For compound **3**, although the emission  $\lambda_{\text{max}}$  was not affected by solvent polarity, its shoulder peak at ~540 nm experiences broadening and a red-shift with increasing solvent polarity which is consistent with the involvement of both  $\pi \rightarrow \pi^*$  and CT transitions for **3**. The absorption and emission profile of **1–4** do not change significantly at the concentration range of 10<sup>-6</sup>–10<sup>-4</sup> M. At concentrations >10<sup>-4</sup> M, the emission spectra of **1**, **2**, and **4** broaden and red-shift, indicating the presence of intermolecular interactions. In contrast, a similar concentration-dependent change was not observed for **3**. In the solid state, compounds **1**, **3**, and **4** display an emission color similar to that observed in solution and have high quantum yields (Table 1 and Figure 4). For **1** and **4**, the solid-state emission spectra are broader and red-shifted by ~10–20 nm compared to their spectra in solution,<sup>9</sup> while the spectrum of **3** experiences no change. Unlike its purple emission in solution, **2** emits a greenish blue color in the solid state with two distinct emission peaks at ~440 and ~500 nm, respectively, where the latter is attributed to the formation of excimers. These observations are consistent with the presence of greater intermolecular interactions for **1**, **2**, and **4**, compared to **3**.

To further understand the fluorescent properties of **1–4**, fluoride titrations employing NBu<sub>4</sub>F (TBAF) in CH<sub>2</sub>Cl<sub>2</sub> were performed (Figure 5). For compounds **1**, **2**, and **4**, a uniform decrease in both the primary absorption bands<sup>9</sup> and emission peaks was observed. This is in agreement with the predicted electronic transitions, as the empty p-orbital of the boron atom is the largest contributor to most of the unoccupied orbitals. Interestingly, the fluorescence of **4** was quenched with fewer equivalents of fluoride compared to **1** and **2**. This may be attributed to the greater steric congestion around the boron atom in **1** and **2** relative to **4**, which is evident in their NMR spectra.<sup>9</sup> As expected from the TD-DFT data, the addition of TBAF to a solution of **3** did not result in complete quenching of the emission peak. Instead, the emission peak is only partially quenched, where the remaining emission peak is likely the result of a localized  $\pi \rightarrow \pi^*$  transition on the indolizino[3,4,5-*ab*]isindole backbone of **3**.

In conclusion, a “one-pot” cycloaddition procedure has been successfully developed for the synthesis of a series of BMes<sub>2</sub>-functionalized N-heterocycles. The boryl unit has been found to greatly diminish intermolecular interactions, rendering the



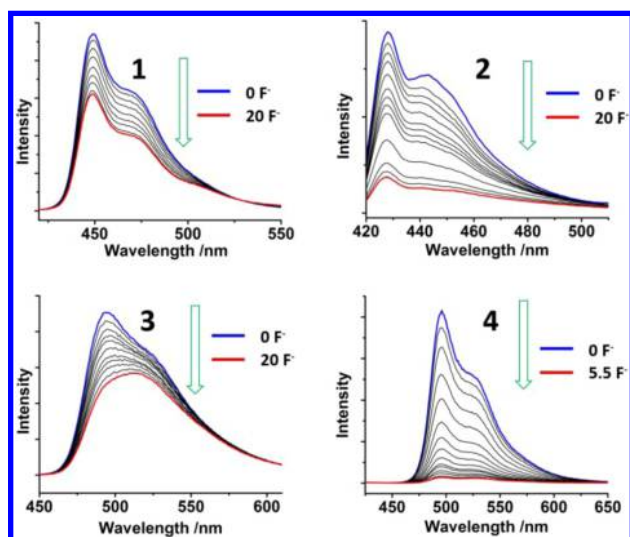


Figure 5. Fluorescent titration of 1–4 ( $10^{-5}$  M) with TBAF in  $\text{CH}_2\text{Cl}_2$  at 298 K.

molecules highly fluorescent with good quantum efficiencies in both solution and the solid state.

## ■ ASSOCIATED CONTENT

### Supporting Information

Figures and tables giving NMR spectra of all compounds, TD-DFT calculation data, all additional UV–vis/fluorescence data of 1–4, and crystal structure data for 1, 1-int, and 3. The Supporting Information is available free of charge on the ACS Publications website at DOI: 10.1021/acs.orglett.5b00994.

## ■ AUTHOR INFORMATION

### Corresponding Authors

\*E-mail: matthias.wagner@chemie.uni-frankfurt.de.

\*E-mail: wangs@chem.queensu.ca.

### Notes

The authors declare no competing financial interest.

## ■ ACKNOWLEDGMENTS

We thank the Natural Sciences and Engineering Research Council (NSERC) of Canada for financial support. S.K.M. thanks NSERC for the Canada Graduate Scholarship (CGS-M). J.R. thanks Das Evangelisches Studienwerk Villigst and Studienstiftung des deutschen Volkes for financial support.

## ■ REFERENCES

- (1) (a) Anthony, J. E. *Chem. Rev.* **2006**, *106*, 5028–5048. (b) Tao, Y.; Yang, C.; Qin, J. *Chem. Soc. Rev.* **2011**, *40*, 2943–2970. (c) Miteva, T.; Meisel, A.; Knoll, W.; Nothofer, H. G.; Scherf, U.; Müller, D. C.; Meerholz, K.; Yasuda, A.; Neher, D. *Adv. Mater.* **2001**, *13*, 565–570. (d) Burroughes, J. H.; Bradley, D. D. C.; Brown, A. R.; Marks, R. N.; Mackay, K.; Friend, R. H.; Burns, P. L.; Holmes, A. B. *Nature* **1990**, *347*, 539–541. (e) He, G.; Pfeiffer, M.; Leo, K.; Hofmann, M.; Birnstock, J.; Pudziel, R.; Salbeck, J. *Appl. Phys. Lett.* **2004**, *85*, 3911–3913.
- (2) (a) Wang, C.; Dong, H.; Hu, W.; Liu, Y.; Zhu, D. *Chem. Rev.* **2012**, *112*, 2208–2267. (b) Wu, W.; Liu, Y.; Zhu, D. *Chem. Soc. Rev.* **2010**, *39*, 1489–1502. (c) Mas-Torrent, M.; Rovira, C. *Chem. Soc. Rev.* **2008**, *37*, 827–838. (d) Zaumseil, J.; Sirringhaus, H. *Chem. Rev.* **2007**, *107*, 1296–1323. (e) Coropceanu, V.; Cornil, J.; da Silva Filho, D. A.; Olivier, Y.; Silbey, R.; Brédas, J.-L. *Chem. Rev.* **2007**, *107*, 926–952. (f) Arias, A. C.;

MacKenzie, J. D.; McCulloch, I.; Rivnay, J.; Salleo, A. *Chem. Rev.* **2010**, *110*, 3–24.

(3) (a) Thomas, S. W., III; Joly, G. D.; Swager, T. M. *Chem. Rev.* **2007**, *107*, 1339–1386. (b) Chen, X.; Pradhan, T.; Wang, F.; Kim, J. S.; Yoon, J. *Chem. Rev.* **2012**, *112*, 1910–1956. (c) Peng, H.; Chen, W.; Cheng, Y.; Hakuna, L.; Strongin, R.; Wang, B. *Sensors* **2012**, *12*, 15907–15946. (d) Kim, J. S.; Quang, D. T. *Chem. Rev.* **2007**, *107*, 3780–3799. (e) Carter, K. P.; Young, A. M.; Palmer, A. E. *Chem. Rev.* **2014**, *114*, 4564–4601.

(4) (a) Mitsumori, T.; Bendikov, M.; Dautel, O.; Wudl, F.; Shioya, T.; Sato, H.; Sato, Y. *J. Am. Chem. Soc.* **2004**, *126*, 16793–16803. (b) Hu, H.; Li, G.; Hu, W.; Liu, Y.; Wang, X.; Kan, Y.; Ji, M. *Org. Lett.* **2015**, *17*, 1114–1117. (c) Matsuda, Y.; Gotou, H.; Katou, K.; Matsumoto, H.; Yamashita, M.; Takahashi, K.; Ide, S. *Heterocycles* **1990**, *31*, 983–986. (d) Liu, Y.; Hu, H.-Y.; Zhang, Y.; Hu, H.-W.; Xu, J.-H. *Org. Biomol. Chem.* **2010**, *8*, 4921–4926. (e) Tominaga, Y.; Shiroshita, Y.; Hosomi, A. *Heterocycles* **1988**, *27*, 2251–2288.

(5) (a) Hudson, Z. M.; Wang, S. *Acc. Chem. Res.* **2009**, *42*, 1584–1596. (b) Jäkle, F. *Chem. Rev.* **2010**, *110*, 3985–4022. (c) Bissinger, P.; Steffen, A.; Vargas, A.; Dewhurst, R. D.; Damme, A.; Braunschweig, H. *Angew. Chem., Int. Ed.* **2015**, *54*, 4362–4366. (d) Marwitz, A. J. V.; Jenkins, J. T.; Zakharov, L. N.; Liu, S. Y. *Angew. Chem., Int. Ed.* **2010**, *49*, 7444–7447. (e) Matsuo, K.; Saito, S.; Yamaguchi, S. *J. Am. Chem. Soc.* **2014**, *136*, 12580–12583. (f) Kushida, T.; Camacho, C.; Shuto, A.; Irle, S.; Muramatsu, M.; Katayama, T.; Ito, S.; Nagasawa, Y.; Miyasaka, H.; Sakuda, E.; Kitamura, N.; Zhou, Z.; Wakamiya, A.; Yamaguchi, S. *Chem. Sci.* **2014**, *5*, 1296–1304. (g) Entwistle, C. D.; Marder, T. B. *Angew. Chem., Int. Ed.* **2002**, *41*, 2927–2931. (h) Entwistle, C. D.; Marder, T. B. *Chem. Mater.* **2004**, *16*, 4574–4585. (i) Ji, L.; Edkins, R. M.; Sewell, L. J.; Beeby, A.; Batsanov, A. S.; Fucke, K.; Drafz, M.; Howard, J. A. K.; Moutounet, O.; Ibersiene, F.; Boucekine, A.; Furet, E.; Liu, Z.; Halet, J.-F.; Katan, C.; Marder, T. B. *Chem.—Eur. J.* **2014**, *20*, 13618–13635. (j) Yin, X.; Chen, J.; Lalancette, R. A.; Marder, T. B.; Jäkle, F. *Angew. Chem., Int. Ed.* **2014**, *53*, 9761–9765. (k) Zhang, Z.; Edkins, R. M.; Nitsch, J.; Fucke, K.; Eichhorn, A.; Steffen, A.; Wang, Y.; Marder, T. B. *Chem.—Eur. J.* **2015**, *21*, 177–190.

(6) (a) Wade, C. R.; Broomsgrove, A. E. J.; Aldridge, S.; Gabbai, F. P. *Chem. Rev.* **2010**, *110*, 3958–3984. (b) Zhao, H.; Leamer, L. A.; Gabbai, F. P. *Dalton Trans.* **2013**, *42*, 8164–8178. (c) Bresner, C.; Haynes, C. J. E.; Addy, D. A.; Broomsgrove, A. E. J.; Fitzpatrick, P.; Vidovic, D.; Thompson, A. L.; Fallis, I. A.; Aldridge, S. *New J. Chem.* **2010**, *34*, 1652–1659.

(7) Yang, D.-T.; Møllerup, S. K.; Wang, X.; Lu, J.-S.; Wang, S. *Angew. Chem., Int. Ed.* **2015**, *54*, 5498–5501.

(8) (a) Kajigaeshi, S.; Mori, S.; Fujisaki, S.; Kanemasa, S. *Bull. Chem. Soc. Jpn.* **1985**, *58*, 3547–3551. (b) Bertermann, R.; Braunschweig, H.; Brown, C. K. L.; Damme, A.; Dewhurst, R. D.; Hörl, C.; Kramer, T.; Krummenacher, I.; Pfaffinger, B.; Radacki, K. *Chem. Commun.* **2014**, *50*, 97–99. (c) Fukazawa, A.; Yamada, H.; Yamaguchi, S. *Angew. Chem., Int. Ed.* **2008**, *47*, 5582–5585. (d) An, Z.; Odom, S. A.; Kelley, R. F.; Huang, C.; Zhang, X.; Barlow, S.; Padilha, L. A.; Fu, J.; Webster, S.; Hagan, D. J.; Van Stryland, E. W.; Wasielewski, M. R.; Marder, S. R. *J. Phys. Chem. A* **2009**, *113*, 5585–5593.

(9) See the Supporting Information for details.

(10) Li, X.; Li, C.; Yin, B.; Li, C.; Liu, P.; Li, J.; Shi, Z. *Chem.—Asian J.* **2013**, *8*, 1408–1411 and references cited therein.

(11) (a) Caramella, P.; Houk, K. N. *J. Am. Chem. Soc.* **1976**, *98*, 6397–6399. (b) Caramella, P.; Gandour, R. W.; Hall, J. A.; Deville, C. G.; Houk, K. N. *J. Am. Chem. Soc.* **1977**, *99*, 385–392.

(12) Zhao, S. B.; Wucher, S. B.; Hudson, Z. M.; McCormick, T. M.; Liu, X. Y.; Wang, S.; Feng, X. D.; Lu, Z. H. *Organometallics* **2008**, *27*, 6446–6456.